Apical sorting of a voltage- and Ca^{2+}-activated K^+ channel α-subunit in Madin-Darby canine kidney cells is independent of N-glycosylation

Marcela Bravo-Zehnder*†, Patricio Orio‡§, Andrés Norambuena*†, Martin Wallner¶, Pratap Meera¶, Ligia Toro‖, Ramón Latorre‡§, and Alfonso González*†††‡‡**

*Departamento de Inmunología Clínica y Reumatología, Facultad de Medicina, †Departamento de Biología Celular y Molecular, **Centro de Regulación Celular y Patología, Facultad de Ciencias Biológicas, Pontificia Universidad Católica de Chile, and ††Millennium Institute for Fundamental and Applied Biology, Casilla 114-D Santiago, Chile; ‡Departamento de Biología, Facultad de Ciencias, Universidad de Chile, and §Centro de Estudios Científicos, Casilla 1469 Valdivia, Chile; and Departments of ¶Anesthesiology and ‖Molecular and Medical Pharmacology, and Brain Research Institute, University of California, Los Angeles, CA 90095-1778

The voltage- and Ca^{2+}-activated K^+ ($K_{V,Ca}$) channel is expressed in a variety of polarized epithelial cells seemingly displaying a tissue-dependent apical-to-basolateral regionalization, as revealed by electrophysiology. Using domain-specific biotinylation and immunofluorescence we show that the human channel $K_{V,Ca}$ α-subunit (human *Slowpoke* channel, h*Slo*) is predominantly found in the apical plasma membrane domain of permanently transfected Madin-Darby canine kidney cells. Both the wild-type and a mutant h*Slo* protein lacking its only potential N-glycosylation site were efficiently transported to the cell surface and concentrated in the apical domain even when they were overexpressed to levels 200- to 300-fold higher than the density of intrinsic *Slo* channels. Furthermore, tunicamycin treatment did not prevent apical segregation of h*Slo*, indicating that endogenous glycosylated proteins (e.g., $K_{V,Ca}$ β-subunits) were not required. h*Slo* seems to display properties for lipid-raft targeting, as judged by its buoyant distribution in sucrose gradients after extraction with either detergent or sodium carbonate. The evidence indicates that the h*Slo* protein possesses intrinsic information for transport to the apical cell surface through a mechanism that may involve association with lipid rafts and that is independent of glycosylation of the channel itself or an associated protein. Thus, this particular polytopic model protein shows that glycosylation-independent apical pathways exist for endogenous membrane proteins in Madin-Darby canine kidney cells.

human *Slowpoke* channel | epithelial polarity

Polarized epithelial cells accomplish vectorial functions of transport, absorption, and secretion based on their morphologically and functionally distinct apical and basolateral cell surface domains that contain different protein and lipid compositions (1, 2). Continuous segregation of specific proteins into each domain is directed by sorting signals encoded in the structure of the transported protein (1). Basolateral sorting signals are confined to discrete cytosolic segments of transmembrane proteins, frequently involving critical tyrosine or dileucine residues and probably decoded by different cytosolic adaptors (3, 4). For apical destination, the mechanisms and the identification of sorting information have remained more elusive and controversial (1, 2). Apical sorting signals can reside in extracellular, membrane-anchoring, and/or cytosolic domains of the transported proteins, and can be encoded or functionally depend on glycosylphosphatidylinositol (GPI) anchors, N- and O-glycans, and proteinaceous patches (1, 5–8). GPI anchors (9, 10) and certain transmembrane domains (6) seem to act as apical sorting signals through interaction with lipid rafts. Lipid rafts are liquid-ordered membrane microdomains rich in cholesterol and glycosphingolipids that serve as platforms or converging centers for decoding apical sorting information (1, 11). Other transmembrane domains direct apical destination without raft association (5). Apical sorting information also is found in the cytosolic domain of polytopic proteins (7, 8, 12), suggesting decoding mechanisms similar to those of basolateral membrane proteins.

An aspect under intense scrutiny deals with the hypothesis that N-glycans are ubiquitous apical sorting signals presumably recognized by cellular lectins at the trans-Golgi network (1, 13–15). However, an alternative hypothesis based on a balanced consideration of the evidence, is that both N- and O-glycans play an indirect facilitative role by providing structural support for functional expression of proteinaceous apical sorting signals (1). To further understand apical sorting mechanisms it is important to find and characterize apical pathways not mediated by glycans, especially in transmembrane proteins endogenous to epithelial cells.

Ion channels of ubiquitous expression have remained relatively unexplored as substrates of the protein sorting machinery in polarized epithelial cells (16–18). The high-conductance, voltage-dependent, Ca^{2+}-sensitive potassium channel ($K_{V,Ca}$) expressed in a variety of epithelial cells and neurons (19) is an interesting model system to address yet poorly understood aspects of polarized protein sorting, including the role of N-glycans in polytopic membrane proteins. A complex of at least two subunits forms $K_{V,Ca}$ channels, the pore-forming α-subunit and the regulatory β-subunits, β1–β4 (20–25). The α-subunit is the product of a single gene, which produces isoforms by alternative splicing and consists of seven N-terminal transmembrane segments (S0–S6) and a large C terminus encompassing two-thirds of the molecule with four hydrophobic regions (S7–S10) (26). A single consensus N-glycosylation site is located within a short loop between S3 and S4. The β-subunits are N-glycosylated and, with the exception of a β3 isoform, endow the channel with altered kinetics, calcium/voltage, and toxin sensitivities (23–25). In a diversity of epithelial cells, from kidney (27–29), male reproductive tract (30), oviduct (31), and vestibulum (32), $K_{V,Ca}$ channels have been electrophysiologically detected at the apical domain. However, they have been also reported in the basolateral domain of enterocytes (33) and

Abbreviations: h*Slo*, human *Slowpoke* channel; $K_{V,Ca}$, Ca^{2+}-sensitive voltage-dependent K^+ channel; MDCK, Madin-Darby canine kidney; EGFR, epidermal growth factor receptor; ER, endoplasmic reticulum.

epithelial cells from acinar glands (34). Proteins can hold both apical and basolateral signals, acting in such a hierarchical fashion that basolateral signals usually are dominant (3). Which sorting information could be present in the $K_{V,Ca}$ channel α-subunit and how it is decoded in different cell types remains unknown.

In Madin-Darby canine kidney (MDCK) cells, which presumably are derived from the transporting kidney epithelial cells of the distal tubule and early portion of the collecting duct, the $K_{V,Ca}$ channels have been detected only apically by electrophysiology (27, 28). We have overexpressed recombinant $K_{V,Ca}$ channel α-subunit (human *Slowpoke* channel, h*Slo*) bearing an N-terminal c-myc epitope in permanently transfected MDCK cells to assess its regionalization and molecular sorting mechanisms at the protein level. We found that h*Slo* is effectively targeted to the apical membrane. In contrast with most membrane proteins, both its transport to the cell surface and apical segregation do not require glycosylation, neither of itself nor of a β-subunit. Its intrinsic proteinaceous apical information might be functionally expressed through association with lipid rafts.

Materials and Methods

Expression Plasmids and Site-Directed Mutagenesis. The h*Slo* cDNA (GenBank accession no. U11058) tagged with c-myc epitope inserted into the pcDNA3 expression vector (Invitrogen) has been described (26). A mutant lacking a possible N-linked glycosylation site between transmembrane segments S3 and S4, was generated with PCR using the overlap extension method (35) to replace Asn-200 with Ala (h*Slo*N200A; GenBank accession no. U11058). A deletion mutant h*Slo*-S0–S6 was made by PCR with primers designed to eliminate all of the carboxyl-terminal region after Ile-323, generating a truncated cDNA, which encodes the S0–S6 region with a stop codon immediately following the predicted S6 transmembrane domain. Mutations were confirmed by dideoxynucleotide chain-termination sequencing (Sequenase, United States Biochemical).

Transfection and Assessment of Protein Expression, Polarity, and Raft Association. pcDNA3 expression plasmids bearing the corresponding cDNAs of h*Slo*, h*Slo*N200A or h*Slo*-S0–S6, preceded by the c-myc epitope, were transfected into type II MDCK cells by using the Lipofectamine plus (GIBCO/BRL) method. Procedures to obtain permanent transformants; assess protein expression by metabolic labeling; determine polarity by domain-specific biotinylation in cells cultured on Transwell chambers, or by indirect immunofluorescence; and measure relative density of fluorograms all have been described (36, 37). Lipid raft association was assessed by isolating low density membrane fractions after either ice-cold detergent extraction or sodium carbonate extraction (100 mM or 500 mM) pH 11 at 4°C for 20 min, as described (38), except that in both cases, floatation of lipid rafts was made on linear sucrose gradients without eliminating cell debris.

Electrophysiology. Currents were measured 1 or 2 days after treatment with 12 mM sodium butyrate, by using the patch-clamp technique in the cell-attached or inside-out configuration (39). Pipettes were pulled from borosilicate glass capillary tubing with filament (Warner Instruments, Hamden, CT). The pipettes had 2–3 megohm resistances. Currents in MDCK cells were recorded by using pipettes filled with: 10 mM NaOH, 141 mM KOH, 151 mM methanesulfonic acid, 1 mM $CaCl_2$, 1 mM $MgCl_2$, 10 mM glucose, 10 mM Hepes, pH 7.3. For the bath solution, $CaCl_2$ was replaced by 5 mM EGTA. Ca^{2+} concentration, adjusted by adding concentrated $CaCl_2$, was measured with a Ca^{2+} electrode (World Precision Instruments, Sarasota, FL) (40). The current signal was digitized to a frequency equal to 5-fold the filter cutoff frequency. Acquisition and basic analysis of the data were carried out with PCLAMP 6.0 software (Axon Instruments, Foster City, CA).

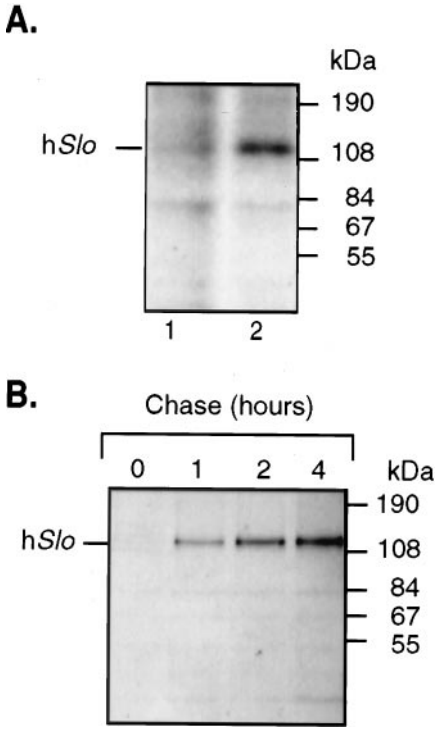

Fig. 1. Expression and kinetics of cell surface appearance of h*Slo* in permanently transfected MDCK cells. (*A*) MDCK cells ($1–2 \times 10^6$ cells), permanently transfected with c-myc-tagged h*Slo*, were incubated 24 h in the absence (lane 1) or presence (lane 2) of 12 mM sodium butyrate to induce h*Slo* expression. Subsequently, cells were metabolically labeled with 200 μCi/ml [^{35}S]methionine-cysteine for 30 min. Immunoprecipitation of h*Slo* was made with anti-c-myc antibody. Proteins were resolved in SDS/PAGE and visualized by fluorography. (*B*) Cells previously treated with sodium butyrate were pulse-labeled for 30 min and chased for the indicated time periods. Cells then were incubated at 4°C with anti-c-myc antibody for 1 h to bind the newly synthesized h*Slo* that reached the cell surface. Immunoprecipitation was performed after cell lysis by using Protein A-Sepharose. The recombinant h*Slo* already was detected at the cell surface within the first hour of chase.

Results

Overexpressed h*Slo* Is Efficiently Transported to the Cell Surface and Apically Segregated in MDCK Cells. A recombinant c-myc-tagged human $K_{V,Ca}$ channel α-subunit (h*Slo*) (26) was overexpressed in permanently transfected MDCK cells upon induction with sodium butyrate. It migrates in SDS/PAGE as a 116-kDa protein easily detectable by metabolic labeling and immunoprecipitation (Fig. 1*A*). Pulse–chase experiments, in which the cells were metabolically labeled for 30 min with [^{35}S]methionine-cysteine and then chased for different time periods, showed that the newly synthesized protein is rapidly transported and inserted into the exposed apical plasma membrane. h*Slo* was already immune-detected at the cell surface within the first hour of chase (Fig. 1*B*). This strategy to study h*Slo* channel sorting was used because the number of h*Slo* channels in MDCK cells has been estimated as 145 per cell (27). This amount is under the limit of detection by techniques currently used to study polarity at the protein level.

h*Slo* in the apical and basolateral domains of transfected MDCK cells was quantitatively assessed by domain-specific biotinylation of cells forming impermeable monolayers on Transwell chambers. More than 90% of the protein was apically distributed (Fig. 2*A*, lanes 1 and 2). Instead, the epidermal

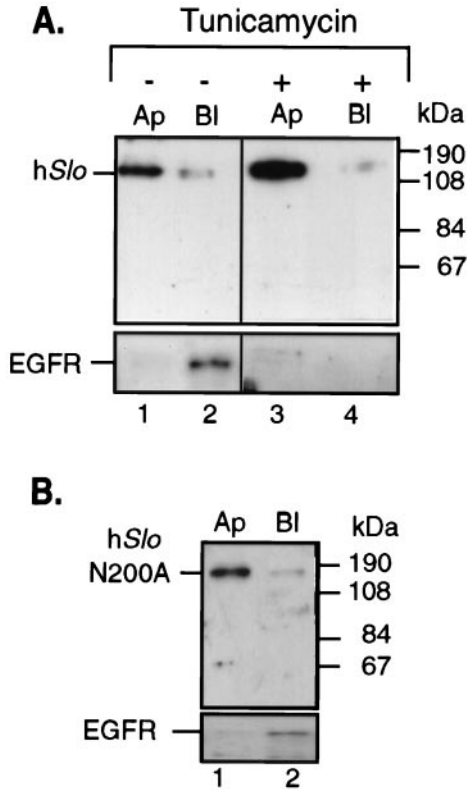

Fig. 2. Apical sorting of the h*Slo* α-subunit does not require N-glycosylation. Permanent transfectants of MDCK cells expressing either the wild-type h*Slo* (*A*) or the mutant *hSlo* N200A that lacks the only possible N-glycosylation site (*B*), were grown in Transwell chambers to form impermeable monolayers. The apical (Ap) and basolateral (Bl) distribution of the overexpressed h*Slo* and the endogenous EGFR were assessed by cell surface domain-specific biotinylation, followed by streptavidin precipitation, SDS/PAGE, and immunoblot with anti-myc or anti-EGFR antibodies. (*A*) The cells were treated in the absence (lanes 1 and 2) or presence (lanes 3 and 4) of 12 μg/ml tunicamycin for 18 h. h*Slo* treated and untreated with tunicamicyn and h*Slo*-N200A distributed more than 90% apical, whereas the EGFR was predominantly basolateral in the same cells. Note that the long treatment with tunicamycin diminished the amount of EGFR at the cell surface but did not affect the apical distribution of h*Slo*.

growth factor receptor (EGFR) was found more than 90% basolateral.

Glycosylation Does Not Determine the Apical Sorting of h*Slo*. The membrane topology proposed for the $K_{V,Ca}$ channel α-subunit (26) showed that three residues linking transmembrane segments S3 and S4 constitute the only suitable extracellular consensus N-glycosylation site. This loop seems too short to be N-glycosylated, as suggested by extensive analysis of a large number of multispan membrane glycoproteins (41). Nevertheless, we have used two experimental approaches to rule out the possibility that N-glycosylation is involved in apical delivery of h*Slo*. Long-term treatment with tunicamycin did not affect either the apical distribution or the cell surface expression of the h*Slo* protein (Fig. 2*A*, lanes 2 and 3) but provoked a decrease of the EGFR at the basolateral surface. Most membrane proteins do not reach the cell surface when N-glycosylation is inhibited (14). In addition, we eliminated its only potential N-glycosylation site. This mutant *hSlo*-N200A was found apically distributed with similar efficiency as the wild-type protein (Fig. 2*B*).

In wild-type MDCK cells and in transfected cells not induced by sodium butyrate, we could hardly detect macroscopic h*Slo* channel currents. However, butyrate treatment of MDCK cells

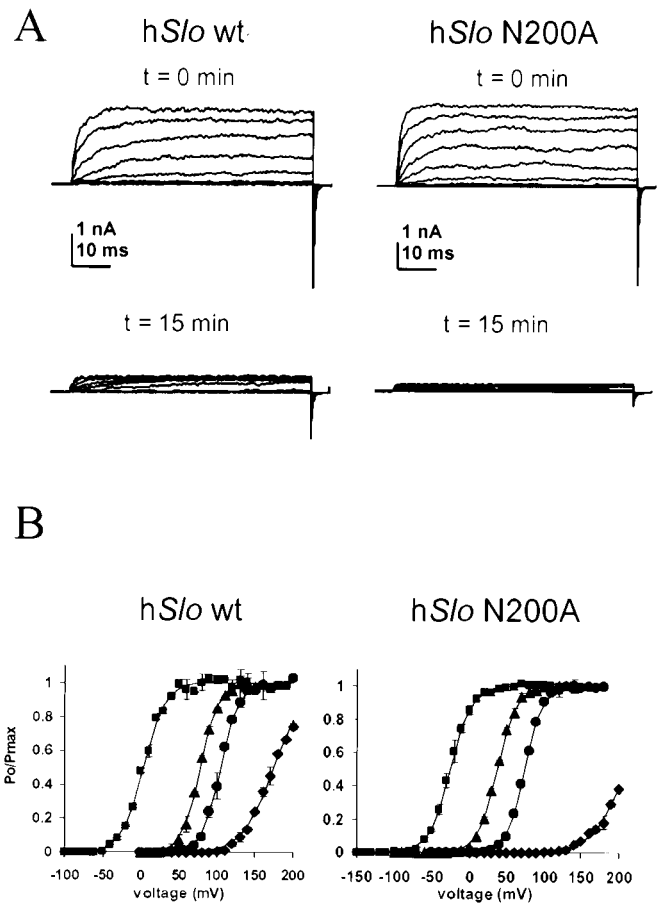

Fig. 3. Electrophysiological characterization of overexpressed hSlo and mutant hSlo-N200A channels at the apical cell surface of transfected MDCK cells. (*A*) Examples of macroscopic currents from wild-type h*Slo* and N200A channels. A voltage pulse protocol consisting in voltage steps of 30 mV applied from a holding voltage of 0 mV in the range of 0 to 270 mV was given immediately after seal formation (0 min) and 15 min after. In both cases, after 15 min 20 nM iberiotoxin in the pipette blocked the h*Slo* and the N200A mutant channels. (*B*) h*Slo* channel normalized open probability ($P_o/P_{o\ max}$) values were obtained from normalized tail currents (I/I_{max}) at the indicated voltages. Each graph corresponds to a single inside-out patch that was exposed to different Ca^{2+} concentrations and is representative of at least three different patches. Solid lines show least-squares fits to Boltzmann equation: $I_{tail} = I_{tail(max)}/\{1 - \exp[-(z_{eq}F(V-V_{1/2})]/(RT)\}$, where V is the test pulse potential, z_{eq} is the apparent number of gating charges, $V_{1/2}$ is the half-activation potential and F, R, and T are faraday constant, gas constant, and absolute temperature, respectively. For 200 nM, 800 nM and 30 μM Ca^{2+}, $V_{1/2}$ values obtained for *hSlo* channels were (in mV; average $\pm$ SD): 104.8 $\pm$ 1.2, 78.1 $\pm$ 0.5, and 3.2 $\pm$ 0.9, respectively. z_{eq} values were 2.13 $\pm$ 0.16, 2.12 $\pm$ 0.12, and 1.77 $\pm$ 0.2, respectively. For *hSlo* N200A channels, $V_{1/2}$ values were 74.3 $\pm$ 0.8, 37.2 $\pm$ 0.6, and $-$ 25.4 $\pm$ 1.8; and z_{eq} values were 2.17 $\pm$ 0.07, 2.01 $\pm$ 0.08, and 1.84 $\pm$ 0.02, respectively.

expressing *hSlo* or *hSlo*-N200A led to detection of robust macroscopic h*Slo* channel currents that were almost completely blocked by iberiotoxin, a specific blocker for h*Slo* channels (Fig. 3*A*) (42). From the maximum conductance and single-channel conductance of 230 pS, we estimated a range of 250 to 350 channels per patch under overexpression conditions. The voltage- and calcium-dependence of both h*Slo* and h*Slo*-N200A (Fig. 3*B*) were in reasonable agreement to those for h*Slo* expressed alone, without a regulatory β-subunit, in oocytes (40).

Association of Nonglycosylated h*Slo* with Lipid Rafts. Lipid rafts enriched in glycosphingolipids and cholesterol are currently

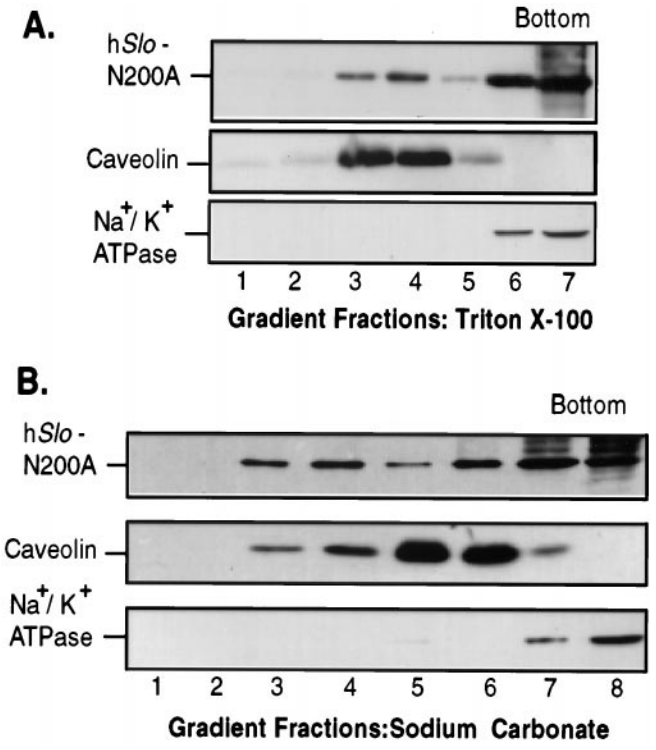

Fig. 4. Gradient density floatation of the hSlo-N200A in transfected MDCK cells. To assess raft association of h*Slo*-N200A, transfected MDCK cells were extracted either with 1% Triton X-100 at 4°C (*A*) or 500 mM sodium carbonate pH (*B*). Lysates were centrifuged to equilibrium in a linear sucrose gradient to isolate lipid rafts by floatation. Fractions were harvested from the bottom of the gradient, and aliquots were precipitated with 20% trichloroacetic acid and subjected to SDS/PAGE and immunoblot analysis. Proteins were visualized by ECL. (*A*) h*Slo*-N200A was detected floating in lighter buoyant densities together with the endogenous raft-marker caveolin-1. (*B*) High-salt treatment did not prevent floatation of h*Slo*-N200A that occurred mostly in fractions 3 and 4. The bulk of caveolin-1 is seen floating in fractions 5 and 6. Na^+/K^+ ATPase, used as a negative control of no association with lipid rafts, did not float and was recovered at the bottom of the gradient.

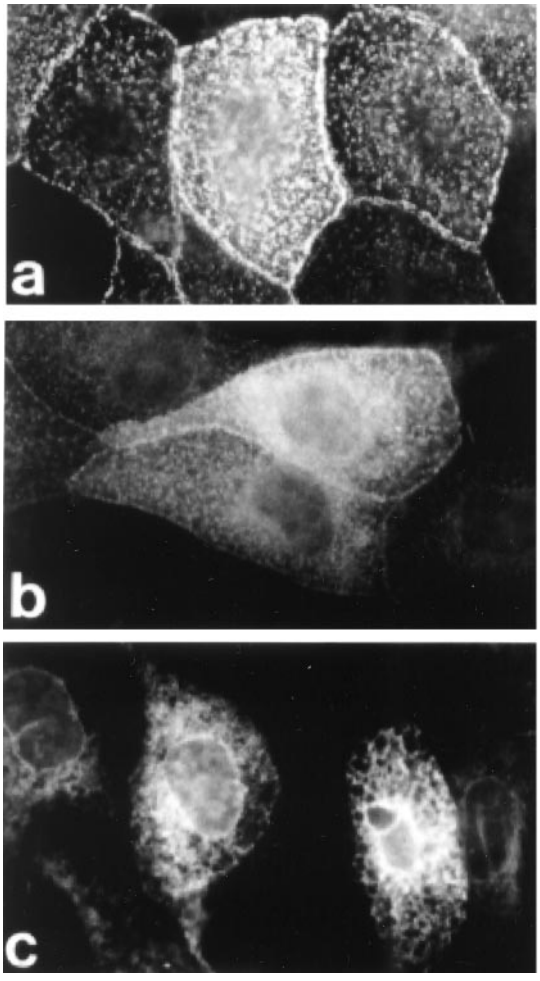

Fig. 5. Immunofluorescence of c-myc-tagged h*Slo* and the truncated mutant h*Slo*-S0–S6. Permanently transfected MDCK cells were grown on coverslips, treated with 12 mM sodium butyrate for 48 h, and fixed with 4% paraformaldehyde. Nonpermeabilized cells (*a*) and cells permeabilized with 0.2% Triton X-100 (*b* and *c*) were subjected to indirect immunofluorescence staining with anti-c-myc monoclonal antibody. h*Slo* shows a predominantly apical distribution (*a* and *b*), with a scant immune reaction inside the cell. Instead, the truncated mutant bearing a deletion after S6 (*hSlo*-S0–S6) showed no staining at the cell surface in nonpermeabilized cells (not shown), but revealed an intense intracellular reticular pattern characteristic of the ER in permeabilized cells (*c*).

isolated by floatation in sucrose gradients as low-density detergent-resistant membranes (9). After extraction with an excess of ice-cold 1% Triton X-100 for 20 min, a proportion of the h*Slo*-N200A was consistently found floating in low-density fractions together with the raft marker caveolin-1 (Fig. 4*A*). Because the stability of the interaction of h*Slo*-N200A with lipid rafts to detergent extraction might be low, we also have used an alternative detergent-free method for lipid raft isolation based on sodium carbonate extraction at pH 11 (38). This procedure showed more h*Slo*-N200A floating in low buoyancy fractions (Fig. 4*B*). Similar results were obtained at 100 mM or 500 mM sodium carbonate. As a negative control, the endogenous Na^+/K^+ ATPase that does not associate with rafts (5, 38) was completely distributed toward the bottom of sucrose gradients (Fig. 4). These results suggest that h*Slo* has properties for being targeted to lipid raft microdomains.

Transport of h*Slo* Protein to the Cell Surface Requires the Carboxyl-Terminal Region. The primary sequence of the h*Slo* shows seven transmembrane domains (S0–S6) and a large COOH terminus (26, 43), which in principle might hold structural information for apical segregation, as reported for several polytopic proteins (7, 8, 12). Therefore, we made a mutant truncated immediately after the S6 transmembrane region (h*Slo*-S0–S6). This mutant protein lost capability for transport to the cell surface, being instead retained in the endoplasmic reticulum (ER) and degraded. Indirect immunofluorescence revealed most of the h*Slo* at the apical cell surface, showing the characteristic punctate staining pattern of microvilli (Fig. 5 *a* and *b*), without a large intracellular pool (Fig. 5*b*). In contrast, the truncated h*Slo*-S0–S6 was not detected at the cell surface but instead showed the characteristic ER reticular pattern (Fig. 5*c*). After metabolically labeling the cells overnight and chasing, the h*Slo* protein decayed with a half-life of about 15–20 h whereas h*Slo*-S0-S6 almost disappeared after 6–12 h of chase (Fig. 6). Thus, for reasons remaining to be elucidated, deletion of such COOH-terminal region impaired h*Slo* exocytic transport.

Discussion

In the present work, we found evidence indicating that the $K_{V,Ca}$ channel α-subunit possesses intrinsic molecular properties to be transported along the exocytic route and sorted to the apical plasma membrane domain of MDCK cells. Its sorting mechanism was independent of both glycosylation and coexpression

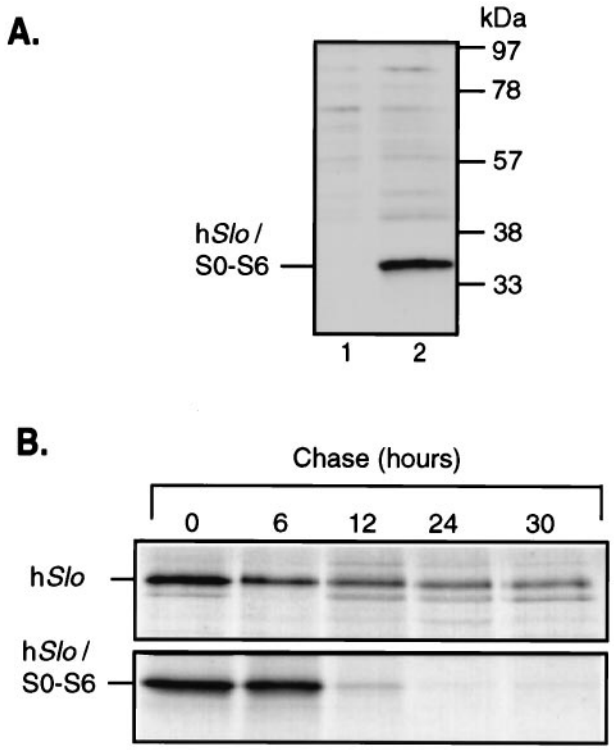

Fig. 6. Truncated hSlo-S0–S6 has a decreased half-life compared with hSlo. (*A*) Synthesis of the c-myc-tagged truncated protein h*Slo*-S0–S6 (37 kDa) induced by sodium butyrate. ^{35}S labeling and immunoprecipitation was as in Fig. 1*A*. (*B*) Transfected MDCK cells expressing either h*Slo* or the truncated h*Slo*-S0–S6 were labeled with 100 μCi/ml [^{35}S]methionine-cysteine for 18 h and then chased for the indicated times. The calculated half-life of h*Slo* was about 16 h whereas the h*Slo*-S0–S6 disappeared abruptly between 6 and 12 h of chase.

with a β-subunit. This particular polytopic model protein provides evidence that endogenous membrane proteins in MDCK cells can use glycosylation-independent apical sorting pathways.

Cell surface delivery of other polytopic proteins, such as some ion pumps (44) and voltage-dependent K^+ channels (45), requires or is enhanced by membrane bound or soluble cytosolic β-subunits, respectively. Also, β-subunit isoforms may critically influence polarity as recently described for the Na^+/K^+ ATPase in polycystic kidney (46). It is not known which β-subunit isoform or isoforms of the $K_{V,Ca}$ channel are expressed in MDCK cells. However, the kinetics of current activation, the values for half-activation voltage ($V_{1/2}$), and the sensitivity to iberiotoxin, correspond to the channel activity of the h*Slo* in the absence of β1-, β2-, or β4-subunits (23–25). Moreover, the results with tunicamycin argue against the possibility that apical sorting of the nonglycosylated *hSlo* could be mediated by interaction with an endogenously expressed N-glycosylated β-subunit that does not alter channel kinetics or $V_{1/2}$ values, like a β3 subunit isoform (24, 25). It also seems unlikely that the h*Slo* overexpression levels achieved by our transfected cells could have been matched by any endogenous β-subunit.

N-linked glycosylation is essential for apical delivery of a variety of secretory and membrane proteins whose exit from the ER, transport to the cell surface, and apical expression can fail when N-glycosylation is inhibited or abrogated by mutation (14). This is not the case for h*Slo* because neither tunicamycin treatment nor mutation of the single N-glycosylation site changed its apical segregation. Furthermore, none of the extracytoplasmic loops of the h*Slo* display characteristic sequences for O-glycosylation (47), which also could play a role in apical destination (1).

Our present results indicate that polytopic cell membrane proteins can have intrinsic apical sorting information that does not depend on glycosylation to be functional. MAL (myelin and lymphocyte protein), which is necessary for the apical delivery of a number of proteins, is a nonglycosylated polytopic protein that recycles between the trans-Golgi network and the apical plasma membrane (48, 49). Using a viral model protein, we previously have described the existence of an apical secretory pathway mediated by proteinaceous instead of glycan sorting signals (36). More recent evidence has suggested that glycan-mediated and glycan-independent apical sorting mechanisms of secreted proteins compete for a nonlectin apical sorting receptor (50). Because several proteins require N- or O-glycosylation for apical delivery, glycans could act as structural facilitators or stabilizers of apical information encoded in protein conformations (1). The mediation of apical delivery by glycans acting directly as sorting signals (13–15), thus implying the coexistence of lectin-dependent and lectin-independent pathways, remains an open possibility. However, the existence of a lectin sorting-receptor would leave unexplained the examples of nonpolarized sorting of highly glycosylated proteins (1, 37).

Mechanisms invoked for apical sorting include association with lipid raft microdomains (1, 11). N-glycosylation can promote raft association and/or be required in addition to raft association for apical destination (15, 51). However, h*Slo* lacking N-glycosylation seems to possess structural information for both raft association and apical sorting. In fact, h*Slo*-N200A could be detected floating in sucrose gradients after extraction with either detergent or sodium carbonate at densities characteristic for lipid rafts. Specific features present in transmembrane domains could determine association with lipid rafts in variable degrees, reflected in the stability to extraction (6, 52). The role of raft association in the polarity of h*Slo* remains to be elucidated, specially because this property *per se* does not ensure apical sorting in other proteins (6, 15, 53).

In polytopic proteins, apical information has been found in transmembrane (5) and carboxyl-terminal cytosolic domains (7, 8). It is difficult to identify sorting information in multispan membrane proteins, unless a set of isoforms or highly homologous proteins with opposite polarity allow screening by comparison, deletions, and/or mixing domains in hybrid proteins (5, 8). The sorting behavior of other isoforms of hSlo have not been explored. As an initial attempt, we deleted the entire carboxyl-terminal domain after transmembrane segment S6. Unfortunately, a truncated version of h*Slo* encompassing the S0–S6 region lost capability for transport to the cell surface, being instead retained in the ER and degraded. This result was unexpected considering that S1–S6 of h*Slo* share homology with the corresponding regions of other members of the S4 superfamily, such as that of K_V channels (26, 54). Although a bulk traffic of soluble proteins from the ER probably occurs, it is now currently accepted that efficient exit of membrane proteins from the ER is not a default process but is instead selective and must be mediated by information in the cargo protein (55). It is also known that altered folding of newly synthesized proteins in the ER is detected by a quality-control system that leads misfolded proteins to degradation (56). Therefore, the deleted S7–S10 segment may contain structural information for proper folding, assembly, and/or transport to the cell surface.

Apical sorting information in the $K_{V,Ca}$ α-subunit explains its electrophysiological detection in the apical domain of epithelial cells from kidney (27–29), male reproductive tract (30), oviduct (31), and vestibulum (32), but leaves uncertain the mechanism of its basolateral distribution reported in enterocytes (33) and epithelial cells from acinar glands (34). Tissue-specific expression of h*Slo* splice variants might confer variability in the

functional expression or decoding of targeting signals, as reported for K_v channels (18). In addition, it cannot be discarded that, in certain tissues, β-subunit isoforms might determine instead a basolateral location of $K_{V,Ca}$. All of these interesting possibilities should prompt intense future work on the polarized sorting mechanisms of this model protein.

This work received financial support from Fondo Nacional de Investigacion Científica y Tecnologica Grants 1000–0890 (R.L.) and 198-0974 (A.G.), Fondo Nacional/Areas Prioritarias (FONDAP) Grant 13980001, Cátedra Presidencial en Ciencias (R.L. and A.G.), a Human Frontiers in Science Program grant (R.L. and L.T.), National Institutes of Health Grant HL54970 (L.T.), American Heart Association National Center Grant-in-Aid 9750745N (P.M.), and American Heart Association Western States Affiliate Beginning Grant-in-Aid 9960028Y (M.W.). L.T. is an Established Investigator of the American Heart Association. P.O. is recipient of a Doctoral Fellowship from the Andes Foundation. The Millennium Institute for Fundamental and Applied Biology is financed in part by the Ministerio de Planificación y Cooperación de Chile. The Centro de Estudios Científicos is a Millenium Institute.

1. Rodriguez-Boulan, E. & Gonzalez, A. (1999) *Trends Cell Biol.* **9,** 291–294.
2. Mostov, K. E., Verges, M. & Altschuler, Y. (2000) *Curr. Opin. Cell Biol.* **12,** 483–490.
3. Matter, K. & Mellman, I. (1994) *Curr. Opin. Cell Biol.* **6,** 545–554.
4. Folsch, H., Ohno, H., Bonifacino, J. S. & Mellman, I. (1999) *Cell* **99,** 189–198.
5. Dunbar, L. A., Aronson, P. & Caplan, M. J. (2000) *J. Cell Biol.* **148,** 769–778.
6. Lin, S., Naim, H. Y., Chapin Rodriguez, A. & Roth, M. G. (1998) *J. Cell Biol.* **142,** 51–57.
7. Chuang, J. Z. & Sung, C. H. (1998) *J. Cell Biol.* **142,** 1245–1256.
8. Muth, T. R., Ahn, J. & Caplan, M. J. (1998) *J. Biol. Chem.* **273,** 25616–25627.
9. Brown, D. A., Crise, B. & Rose, J. K. (1989) *Science* **245,** 1499–1501.
10. Lisanti, M. P., Caras, I. W., Davitz, M. A. & Rodriguez-Boulan, E. (1989) *J. Cell Biol.* **109,** 2145–2156.
11. Simons, K. & Ikonen, E. (1997) *Nature (London)* **387,** 569–572.
12. Rotin, D., Bar-Sagi, D., O'Brodovich, H., Merilainen, J., Lehto, V. P., Canessa, C. M., Rossier, B. C. & Downey, G. P. (1994) *EMBO J.* **13,** 4440–4450.
13. Scheiffele, P., Peranen, J. & Simons, K. (1995) *Nature (London)* **378,** 96–98.
14. Fiedler, K. & Simons, K. (1995) *Cell* **81,** 309–312.
15. Benting, J. H., Rietveld, A. G. & Simons, K. (1999) *J. Cell Biol.* **146,** 313–320.
16. Le Maout, S., Sewing, S., Coudrier, E., Elalouf, J. M., Pongs, O. & Merot, J. (1996) *Mol. Membr. Biol.* **13,** 143–147.
17. Scannevin, R. H., Murakoshi, H., Rhodes, K. J. & Trimmer, J. S. (1996) *J. Cell Biol.* **135,** 1619–1632.
18. Ponce, A., Vega-Saenz de Miera, E., Kentros, C., Moreno, H., Thornhill, B. & Rudy, B. (1997) *J. Membr. Biol.* **159,** 149–159.
19. Latorre, R., Vergara, C., Stefani, E. & Toro, L. (2000) in *Pharmacology of Ion Channel Functions: Activators and Inhibitors—Handbook of Experimental Pharmacology*, ed. Endo, M. (Springer, Berlin), Vol. 147, pp. 197–223.
20. Knaus, H. G., Folander, K., Garcia-Calvo, M., Garcia, M. L., Kaczorowski, G. J., Smith, M. & Swanson, R. (1994) *J. Biol. Chem.* **269,** 17274–17278.
21. Wallner, M., Meera, P., Ottolia, M., Kaczorowski, G. J., Latorre, R., Garcia, M. L., Stefani, E. & Toro, L. (1995) *Receptors Channels* **3,** 185–199.
22. Wallner, M., Meera, P. & Toro, L. (1999) *Proc. Natl. Acad. Sci. USA* **96,** 4137–4142.
23. Brenner, R., Jegla, T. J., Wickenden, A., Liu, Y. & Aldrich, R. W. (2000) *J. Biol. Chem.* **275,** 6453–6461.
24. Meera, P., Wallner, M. & Toro, L. (2000) *Proc. Natl. Acad. Sci. USA* **97,** 5562–5567.
25. Uebele, V. N., Lagrutta, A., Wade, T., Figueroa, D. J., Liu, Y., McKenna, E., Austin, C. P., Bennett, P. B. & Swanson, R. (2000) *J. Biol. Chem.* **275,** 23211–23218.
26. Meera, P., Wallner, M., Song, M. & Toro, L. (1997) *Proc. Natl. Acad. Sci. USA* **94,** 14066–14071.
27. Bolivar, J. J. & Cereijido, M. (1987) *J. Membr. Biol.* **97,** 43–51.
28. Ponce, A. & Cereijido, M. (1991) *Cell Physiol. Biochem.* **1,** 13–23.
29. Hirsch, J., Leipziger, J., Frobe, U. & Schlatter, E. (1993) *Pflügers Arch.* **422,** 492–498.
30. Sohma, Y., Harris, A., Wardle, C. J., Gray, M. A. & Argent, B. E. (1994) *J. Membr. Biol.* **141,** 69–82.
31. James, A. F. & Okada, Y. (1994) *J. Membr. Biol.* **137,** 109–118.
32. Takeuchi, S., Marcus, D. C. & Wangemann, P. (1992) *Am. J. Physiol.* **262,** C1430–C1436.
33. Burckhardt, B. C. & Gogelein, H. (1992) *Pflügers Arch.* **420,** 54–60.
34. Maruyama, Y., Gallacher, D. V. & Petersen, O. H. (1983) *Nature (London)* **302,** 827–829.
35. Horton, R. M., Cai, Z. L., Ho, S. N. & Pease, L. R. (1990) *BioTechniques* **8,** 528–535.
36. Marzolo, M. P., Bull, P. & Gonzalez, A. (1997) *Proc. Natl. Acad. Sci. USA* **94,** 1834–1839.
37. Gonzalez, A., Rizzolo, L., Rindler, M., Adesnik, M., Sabatini, D. D. & Gottlieb, T. (1987) *Proc. Natl. Acad. Sci. USA* **84,** 3738–3742.
38. Martens, J. R., Navarro-Polanco, R., Coppock, E. A., Nishiyama, A., Parshley, L., Grobaski, T. D. & Tamkun, M. M. (2000) *J. Biol. Chem.* **275,** 7443–7446.
39. Hamill, O. P., Marty, A., Neher, E., Sakmann, B. & Sigworth, F. J. (1981) *Pflügers Arch.* **391,** 85–100.
40. Meera, P., Wallner, M., Jiang, Z. & Toro, L. (1996) *FEBS Lett.* **382,** 84–88.
41. Landolt-Marticorena, C. & Reithmeier, R. A. (1994) *Biochem. J.* **302,** 253–260.
42. Candia, S., Garcia, M. L. & Latorre, R. (1992) *Biophys. J.* **63,** 583–590.
43. Wallner, M., Meera, P. & Toro, L. (1996) *Proc. Natl. Acad. Sci. USA* **93,** 14922–14927.
44. Caplan, M. J. (1998) *Curr. Opin. Cell Biol.* **10,** 468–473.
45. Shi, G., Nakahira, K., Hammond, S., Rhodes, K. J., Schechter, L. E. & Trimmer, J. S. (1996) *Neuron* **16,** 843–852.
46. Wilson, P. D., Devuyst, O., Li, X., Gatti, L., Falkenstein, D., Robinson, S., Fambrough, D. & Burrow, C. R. (2000) *Am. J. Pathol.* **156,** 253–268.
47. Van den Steen, P., Rudd, P. M., Dwek, R. A. & Opdenakker, G. (1998) *Crit. Rev. Biochem. Mol. Biol.* **33,** 151–208.
48. Puertollano, R. & Alonso, M. A. (1999) *Mol. Biol Cell* **10,** 3435–3447.
49. Cheong, K. H., Zacchetti, D., Schneeberger, E. E. & Simons, K. (1999) *Proc. Natl. Acad. Sci. USA* **96,** 6241–6248.
50. Marmorstein, A. D., Csaky, K. G., Baffi, J., Lam, L., Rahaal, F. & Rodriguez-Boulan, E. (2000) *Proc. Natl. Acad. Sci. USA* **97,** 3248–3253.
51. Alfalah, M., Jacob, R., Preuss, U., Zimmer, K. P., Naim, H. & Naim, H. Y. (1999) *Curr. Biol.* **9,** 593–596.
52. Scheiffele, P., Roth, M. G. & Simons, K. (1997) *EMBO J.* **16,** 5501–5508.
53. Lipardi, C., Nitsch, L. & Zurzolo, C. (2000) *Mol. Biol. Cell* **11,** 531–542.
54. Jan, L. Y. & Jan, Y. N. (1992) *Cell* **69,** 715–718.
55. Klumperman, J. (2000) *Curr. Opin. Cell Biol.* **12,** 445–449.
56. Ellgaard, L., Molinari, M. & Helenius, A. (1999) *Science* **286,** 1882–1888.